EXPERIMENTAL AERODYNAMIC PERFORMANCE OF A SELF-TRIMMING WING-SAIL FOR AUTONOMOUS SURFACE VEHICLES

Gabriel Hugh Elkaim * **C. O. Lee Boyce Jr.** **

* *Assistant Professor, UC Santa Cruz, Santa Cruz, CA*
** *Research Assistant, Stanford University, Stanford, CA*

Abstract: Recent experimental testing of an unmanned autonomous marine surface vehicle has demonstrated several key advances for a wind propelled platform. The HWT-X1, is a winged catamaran based on modified conventional sailing vessel intended for use as surveillance and sensor platform in either littoral or unprotected waters. The novel propulsion system is a vertical wing, suspended on bearings and "flown" aerodynamically using conventional flaps and tails. Experimental validation has shown exceptional pointing performance, with upwind progress at 20-25 degrees to the true wind. Additionally, speeds of 60% of the true wind speed are achieved routinely under wind speeds from 12 - 25 knots.

Keywords: Autonomous Surface Vehicle, Wind Propulsion, Wind Polar

1. INTRODUCTION

Autonomous marine surface vehicles (ASV's) have myriad roles in surveillance, littoral patrol, oceanographic sampling, and meteorological investigations (Stambaugh and Thibault, 1992; Fryxell and Silvestre, 1994). The ASV in general can have a much larger sensor footprint than an airborne sensor, as well as having different sensor modalities that can be complementary to the traditional Unmanned Air Vehicle (UAV) platforms. With the addition of wind-based propulsion, energy is scavenged from the environment, allowing for extremely long duration autonomous operation.

Precision guidance and control of an autonomous, wing-sailed catamaran has been demonstrated by the HWT X-1, a modified Stiletto catamaran, capable of tracking straight line segments to better than 1.2 m (1-σ)(Boyce Jr., C.O., and Elkaim, G.H., 2007). This work provides preliminary performance data on the aerodynamic control of the wing as a novel propulsion system for marine surface vehicles. HWT X-1, is a 9.1 m (30 ft) catamaran, with a carbon fiber wing that is 10.7 m (35 ft) tall and has a 3 m (10 ft) chord. For aerodynamic control of the wing (which is free to rotate in azimuth about the stub mast), twin tails are suspended on two carbon fiber booms extending back from the semi-span of the wing, pictured in Fig. 1.

The project is progressing towards environmentally scavenged energy for both propulsion and system power requirements. The wind provides the main propulsive force, and outside of the doldrums near the equator, maintains a reasonable motive force almost anywhere on the oceans. The wing, which is passively stable and self-trimming, is used to propel the vehicle both up and down-

[1] Supported by Harbor Wing Technologies, Inc.

Fig. 1. The HarborWing HWT-X1 experimental prototype wing-sailed autonomous catamaran

wind (though—like all sail boats—not directly into the wind).

2. WING-SAIL PROPULSION

The most visibly unusual feature of HWT X-1 is the vertical wing which replaces the conventional sail, and is the subject of this work. The wind-propulsion system is a rigid wing-sail mounted vertically on bearings that allow free rotation in azimuth about a stub-mast. Aerodynamic torque about the stub-mast is trimmed using two flying tails mounted on booms joined to the wing. This arrangement allows the wing-sail to automatically attain the optimum angle to the wind, and weather vane into gusts without inducing large heeling moments. Modern airfoil design allows for an increased lift to drag ratio (L/D) over a conventional sail, thus providing thrust while reducing the overturning moment and higher pointing ability. Additionally, by virtue of its rigid surface, the wing-sail is not subject to aeroelastic collapse (luffing) when pointed upwind.

The wing and airfoil section were designed for equivalent performance to the original sail system, low actuation force, and the ability to precisely control the resulting propulsive system. Note that a sloop rig sail can achieve at best a maximum lift coefficient of 0.8 if the jib and sail are perfectly

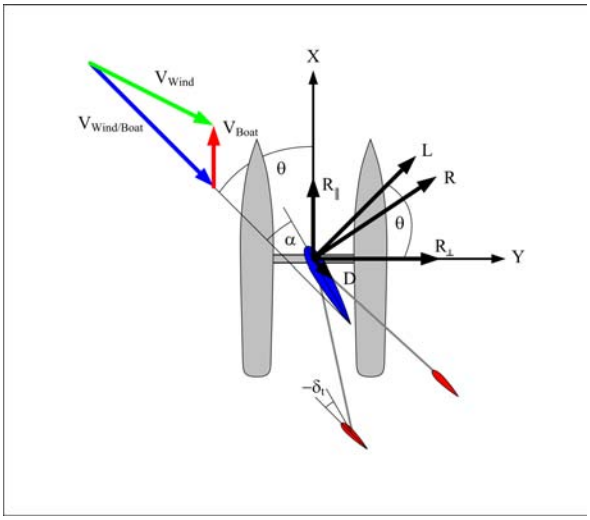

Fig. 2. Beating up wind.

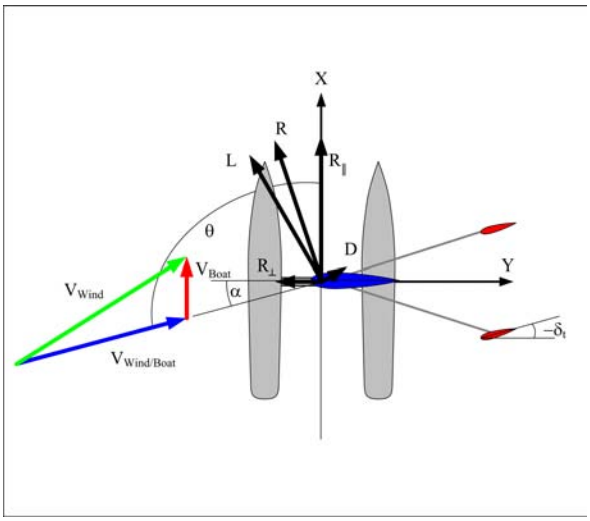

Fig. 3. Reaching across wind.

trimmed (Marchaj, 2002). Realistically, an operating maximum lift coefficient is more likely in the 0.6-0.7 range. Based on computational fluid dynamics modeling using VSAERO (Maskew, 1987) the HWT X-1 wing is predicted to achieve a maximum lift coefficient of 2.2. As this allows the wing to generate three times the force of an equivalently sized sail, the wing area is reduced to one third of the area of the original sails. The distribution of lift is worse for overturning loads due to the aerodynamic loading at the top of the wing (not present on sails due to the extreme taper of conventional sails), however because the drag characteristics of the wing are much improved, the performance of the wing-sailed catamaran should be superior to the original configuration.

2.1 Wing Wind Interaction

While the wing-sail functions similarly to a conventional sail, the wing-sail differs in very fundamental ways from a cloth sail. The most obvious is

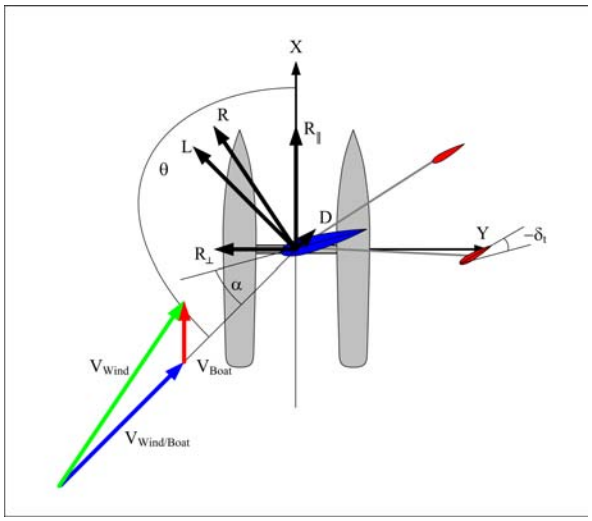

Fig. 4. Running down wind.

that the motion of the wing is completely decoupled from the motion of the hull underneath the wing. Because the wing is controlled aerodynamically from its tails, and due to the bearings that allow the wing to rotate freely in azimuth about the stub mast, the wing flies at a constant angle of attack to the *apparent* wind. That is, if the hull were held fixed, the wing would fly at a constant angle of attack relative to the *true* wind, and that angle of attack would be determined uniquely by the angle of the tails.

The *apparent* wind is the vector sum of the true air motion (wind) and the velocity of the boat. The vector drawing of true wind, apparent wind, and boat velocity is well known and referred to as the *wind triangle*. To illustrate the forces and moments involved with the wing-sail, Figs. 2, 3, and 4 show the forces, velocities, and angles for a port tack (true wind from the forward left), and port reach (true wind from the left side), and a port run (true wind from the left rear), respectively.

In Fig. 2, the HWT X-1 is on a port tack, heading upwind. That is, the true wind is coming from the forward left of the vessel. First, the vessel is stationary with the tails set at 0°, and the wind blowing from the forward port side. The wing-sail will point directly into the wind, and no motion will result. In order to generate forward thrust, the tails are set to an angle of $-\delta_t$, with the leading edge of the tails pointing to the left or aft of the true wind. The airflow past the tails, now at an angle of attack to the wind, causes a force to develop that rotates the entire wing-sail/tail structure clockwise α degrees, effectively unloading the tails. The wing, now at an angle of attack (α) develops lift (L) perpendicular to the true wind, and drag (D) parallel to the true wind (note that the use of lift and drag here is in the conventional aircraft sense). The vector sum of the lift and drag is denoted the resultant (R), which can be resolved into the local body frame as a perpendicular ($R_\perp$) and a parallel ($R_\parallel$) components.

As the boat accelerates, the boat velocity (V_{Boat}) adds in a vector sense to the wind in such a way as to rotate the apparent wind towards the front of the boat. As this happens, the tails react so as to keep the wing-sail angle of attack constant with respect to the apparent wind. Note that this happens regardless of why the apparent wind has changed (change in boat velocity or a change in the true wind direction/velocity). This is why the wing-sail is called self-trimming, as it is passively stable about a fixed angle of attack (Elkaim, 2001).

Fig. 3 shows the vehicle on a port reach, with the wind coming from the left side. The wing-sail functions in exactly the same manner as above, again with the boat velocity rotating the apparent wind forward. On this point of sail, the lift is more closely aligned with $R_\parallel$ thus giving a larger velocity.

Fig. 4 shows the catamaran on a port run, with the wind coming from the rear left side. Again, the function of the wing-sail is identical, and again the boat velocity results in a rotation of the apparent wind towards the front of the boat. It is important to note that here the tails are out in front of boat, rather than in the rear. Again, the angle of attack of the wing-sail is constant. Note that sailing with the wind from the opposite side of the catamaran (starboard) simple requires the tails to be mirrored to a new angle δ_t, which will cause the images and forces to be mirrored as well.

Close inspection of Figs. 2, 3, and 4 will show that the apparent wind is stronger when going upwind, as the resultant of the boat velocity and wind speed is larger than the true wind. When going down wind, the apparent wind is less than the true wind, reducing the available thrust, but also the overturning moment. Also note that when the true wind angle, θ, is less than arctan $\frac{L}{D}$, then the resultant vector is always aft of the beam, and the vessel will slow down to a stop (and in fact, start accelerating backwards, albeit slowly).

2.2 Relationship of Aerodynamic Forces

Aerodynamic force measurements typically require the use of strain gauges and load cells (and often wind tunnels for high quality data). In the interest of time and simplicity, rather than rigging the mast with strain gauges, we used the vessel's roll and the predicted L/D to derive the forces on the wing. From Figs. 2, 3, and 4, we find the following set of equations relate the lift, and drag,

forces to the resultant force components which are parallel and perpendicular to the vessel. The parallel component, $R_{\parallel}$, produces the thrust for the vehicle. Recall that the centerboards prevent the boat from slipping sideways, therefore, the perpendicular component of the resultant, $R_{\perp}$, produces a heeling moment. Eqs. 1 and 2 show the relationship between these forces, where absolute values are used to generalize the equations regardless of point-of-sail.

$$L\,|\sin\theta| - D\cos\theta = R_{\parallel} \tag{1}$$

$$|L\cos\theta + D\,|\sin\theta|\,| = R_{\perp} \tag{2}$$

The heeling force, $R_{\perp}$ is a function of roll angle and can be measured by the vessel's MEMS inertial navigation system. This leaves two equations and three unknowns; therefore, we use the theoretical L/D of 5 predicted by VSAERO to complete the set of equations.

$$L - \frac{1}{L/D}D = 0 \tag{3}$$

Rearranging Eqs. 1 and 2 and substituting in Eq. 3, we arrive at the following form:

$$L = \frac{R_{\perp}}{\left|\cos\theta + \frac{1}{L/D}\,|\sin\theta|\right|} \tag{4}$$

$$D = \frac{L}{L/D}$$

$$R = \sqrt{L^2 + D^2}$$

$$R_{\parallel} = \sqrt{R^2 - R_{\perp}^2}$$

2.3 Roll Calibration

In order to calibrate the heeling force versus roll angle function, the stub mast was loaded horizontally with the wing removed and the displacement of the high hull measured against the waterline. The load was measured using a calibrated load cell, and the hulls were ballasted to compensate for the missing wing. Using this loading data, and the distance between the two hulls, the displacement was converted to a roll angle, and a function fit to the points. The data along with the curve fit is presented in Fig. 5. Note that the increased heel per unit force as the angle of roll increases is consistent with the roll stability of catamarans.

2.4 Power and Reefing of Wing

One of the perceived drawbacks of the wing-sail concept is that the area of the rigid wing cannot be reduced, or reefed, in strong winds. While this

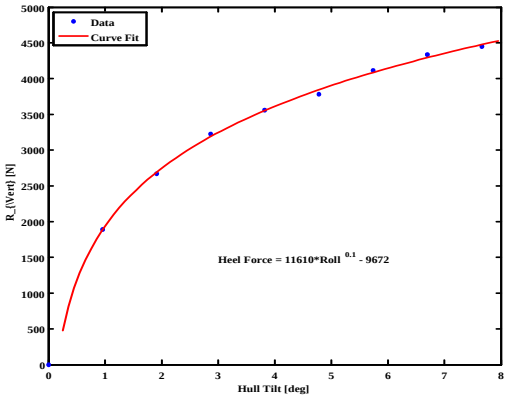

Fig. 5. Data from pull test and curve fit.

is technically true, it is less of an issue than imagined. Firstly, the control over the wing is very precise when compared to a conventional sail. Additionally, because the wing is self-trimming, it self-adjusts to changes in wind directions with a quick rotation, whereas a conventional sail would literally be knocked down by the gust. Also note that based on drag coefficients, the bare mast has much more drag than the wing with the tails set to 0°.

Since the wing flies at constant angle of attack, and that angle of attack is set by the angle of the tails only, reducing the tail angles reduces the power driving the vessel, and thus effectively reefs the wing. Furthermore, as the wing is mass-balanced about the quarter chord, the hulls and the wing are effectively decoupled. The only coupling is the boat velocity, which changes both the speed and direction of the apparent wind.

Another distinction of the wing from a conventional sail is that the lift and drag are controlled independently from the hulls. Because the lift can be flipped to the other side of the apparent wind by switching the angle of the tail (from $+\delta$ to $-\delta$), which causes the angle of attach of the wing to change from $+\alpha$ to $-\alpha$. The resulting reverse thrust allows the vehicle to sail backwards as well as forwards.

3. WING PERFORMANCE

Fig. 6, shows the path of the vehicle off the coast of Ewa beach, Oahu, HI. The vessel follows a course defined by eight waypoints that form a figure-8 pattern. Also denoted is the ground station's location on Ewa beach. Note that the wind was coming from the East, i.e.: blowing from the right side of the figure to the left.

The polar angle, θ, and the angle of attack, α, are plotted for each leg in Fig. 7. Average values for each leg are listed in Table 1. Also, note that

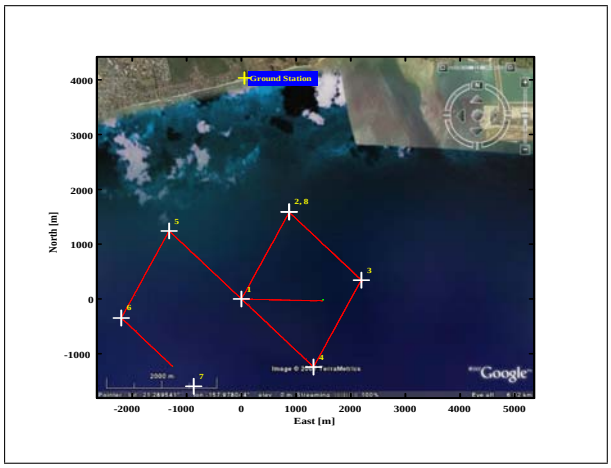

Fig. 6. Path of vehicle, under wind power in open water.

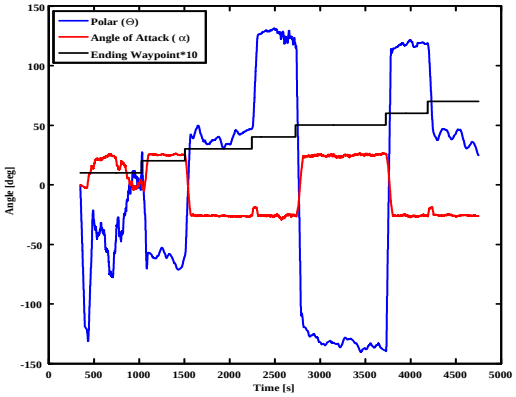

Fig. 7. Wind polar angle and wing angle of attack along open water course segments.

Leg Waypoints	Point of Sail	Polar (θ)	AoA(α)	Roll (ϕ)
1-2	Beat	-61	24	-1.6
2-3	Beat	39	-26	2.7
3-4	Run	124	-26	1.2
4-5	Run	-129	23	0.8
5-6	Run	114	-24	1.5
6-7	Beat	38	-25	3.1

Table 1. Average values over the path segments

the tails were kept at a constant deflection of $\pm 15°$ throughout the course. Fig. 8 shows the smoothed roll data over each course leg.

Roll measurements are small, and as such, they are vulnerable to noise. While running, the heeling force is the difference between lift and drag forces rather than the addition as is the case for beating. Thus Eq. 4, while valid for both traveling up and downwind, gives more reliable results when the vehicle is beating upwind. Fig. 9, shows the calculated lift, drag, and resultant force inferred from the vessel's roll as it transits between waypoints 1 and 3. Lift, five times greater than drag, falls just below the resultant force.

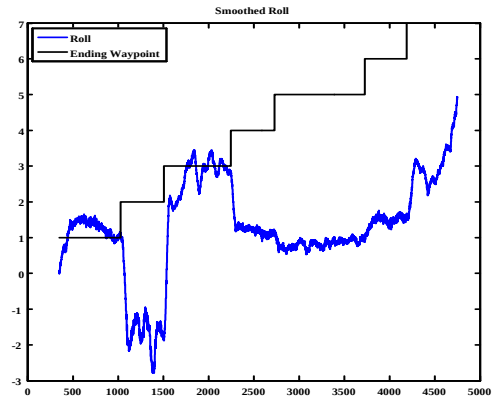

Fig. 8. Smoothed roll angle along open water course segments.

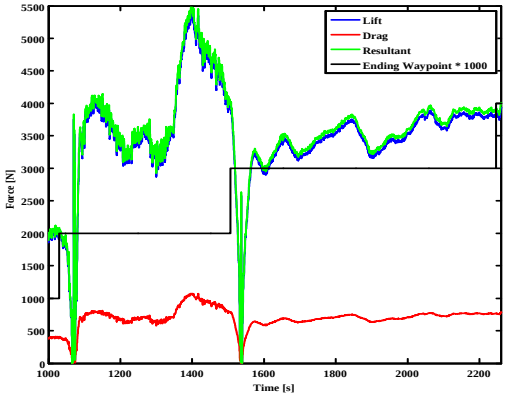

Fig. 9. Lift, drag, and resultant force calculations from wing along open water course segments.

3.1 Coefficient of Lift

Through the measurement of boat roll angle, the aerodynamic forces are derived for the vehicle. Detailed aerodynamic modeling of the wing-sail predicted a performance of a lift to drag ratio (L/D) of 5 at a tail deflection of 15°, with a resulting angle of attack of 30°, and a coefficient of lift of 2.2 (and a coefficient of drag of 0.44). Note that in the Table 1, the measured angle of attack (as measured by the anemometers located in front of the wing) was from 23 to 26°. The discrepancy is most likely due to the upwash from the wing affecting the measurements.

Using the measured wind speed, and the physical parameters of the wing area, $S = 28.3\,\mathrm{m}^2$ ($305\,\mathrm{ft}^2$) and air density $\rho = 1.229\,\mathrm{kg/m}^3$, the coefficient of lift is computed, and plotted in Fig. 10. Note that the wing was experimentally found to have a coefficient of lift of 2.2 which is in agreement with the VSAERO predicted theoretical performance.

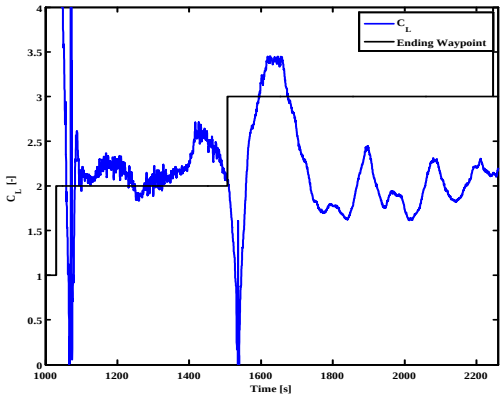

Fig. 10. Coefficient of lift along segments 1-2 and 2-3.

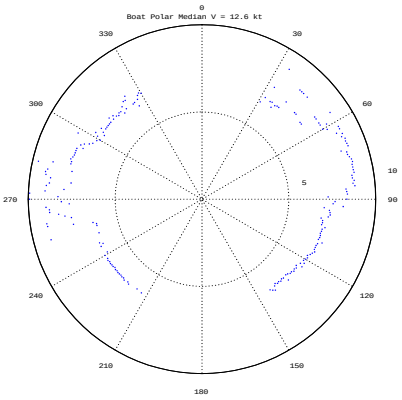

Fig. 11. Experimentally determined performance polar.

3.2 Sailing Polar

Experimental results are taken from sailing data, where both the measured apparent wind and the boat GPS velocity are used to reconstruct the true wind. Using this data, the wing performance is aggregated versus various wind angles, and presented as a ratio of boat velocity to wind velocity. This is what is normally described as a sailing polar. A few key findings are worth highlighting, (1) The HWT X-1 is capable of making progress to wind while pointing 20-25° off of the true wind (at a speed ratio of approximately 0.3), from an angle to the true wind of approximately 45 degrees down to 150 degrees, the speed ratio remains almost constant between 0.5 - 0.6. That is, across the wind, upwind, or down-wind the wing delivers boat speed of 1/2 the speed of the true wind (see Fig. 11).

4. CONCLUSIONS

Using the wind for propulsion of an autonomous marine surface vehicle is a promising technology for long endurance and energy scavenging missions. Utilizing a rigid wing free to rotate about the stub-mast, we have developed a passively stable wing that is decoupled from the hulls beneath, and controlled exclusively by very light actuator loads on flying tails. Using the vehicle roll as a proxy for heeling force, the aerodynamic performance of the wing-sail is estimated. Using a calculated lift to drag ratio (L/D) of 5 from VSAERO modeling, the experimental wing showed a constant angle of attack of 24° with the tails deflected at 15°, and a thrust force of 1000 to 3000 N.

The experimentally calculated coefficient of lift was 2.2, in agreement with the VSAERO predicted value and well in excess of conventional sails at around 0.8. Furthermore, experimental measurements of the wind polar, the ratio of boat speed to true wind speed at various angles to the true wind, show that the wing-sail can propel the boat at 50% to 60% the speed of the true wind on a very large range of angles.

5. ACKNOWLEDGEMENTS

Thanks to Mark Ott and Harbor Wing Technologies for their generous support.

REFERENCES

Boyce Jr., C.O., and Elkaim, G.H. (2007). Control System Performance of an Unmanned Wind-Propelled Catamaran. In: *Proc. Of the IFAC Conference on Control Applications in Marine Systems*. IFAC CAMS. Bol, Croatia.

Elkaim, G. H. (2001). System Identification for Precision Control of a WingSailed GPS-Guided Catamaran. PhD thesis. Stanford University. Stanford, CA.

Fryxell, D., Oliveira P. Pascoal A. and C. Silvestre (1994). An Integrated Approach to the Design and Analysis of Navigation, Guidance and Control Systems for AUVs. In: *Proc. Symposium on Autonomous Underwater Vehicle Technology*. Cambridge, Massachusetts, USA.

Marchaj, C. (2002). *Sail Performance: Techniques to Maximize Sail Power, 2nd Ed.*. International Marine/Ragged Mountain Press. Maine.

Maskew, B. (1987). Program VSAERO Theory Document. Technical Report NASA Contractor Report No. 4023. NASA. Washington, DC.

Stambaugh, J. and R. Thibault (1992). Navigation Requirements for Autonomous Underwater Vehicles. *Journal of the Institute of Navigation* **39**(1), 79–92.